The American Journal of Pathology, Vol. 170, No. 1, January 2007
Copyright © American Society for Investigative Pathology
DOI: 10.2353/ajpath.2007.060497

Matrix Pathobiology

Decorin-Mediated Regulation of Fibrillin-1 in the Kidney Involves the Insulin-Like Growth Factor-I Receptor and Mammalian Target of Rapamycin

Liliana Schaefer,*‡ Wasiliki Tsalastra,* Andrea Babelova,* Martina Baliova,* Jens Minnerup,* Lydia Sorokin,† Hermann-Josef Gröne,§ Dieter P. Reinhardt,¶ Josef Pfeilschifter,‡ Renato V. Iozzo,‖ and Roland M. Schaefer*

From the Departments of Internal Medicine D, and Physiological Chemistry and Pathobiochemistry,† University of Münster, Münster, Germany; Pharmazentrum Frankfurt,‡ Institut fur Allgemeine Pharmakologie und Toxikologie/Zentrum für Arzneimittelsicherheit, Entwicklung und Sicherheit, Klinikum der Johann Wolfgang Goethe-Universität Frankfurt am Main, Frankfurt am Main, Germany; the Department of Cellular and Molecular Pathology,§ German Cancer Research Center, Heidelberg, Germany; the Department of Anatomy and Cell Biology and Faculty of Dentistry,¶ McGill University, Montreal, Quebec, Canada; and the Department of Pathology,‖ Anatomy and Cell Biology, Thomas Jefferson University, Philadelphia, Pennsylvania*

Decorin, a small leucine-rich proteoglycan, affects the synthesis of the elastic fiber component fibrillin-1 in the kidney via hitherto unknown mechanisms. Here, we show that decorin binds to and induces phosphorylation of insulin-like growth factor-I (IGF-I) receptor in renal fibroblasts. Inhibition of the IGF-I receptor tyrosine kinase and its downstream target phosphoinositide-3 kinase prevented decorin-mediated synthesis of fibrillin-1. Furthermore, decorin induced phosphorylation of phosphoinositide-dependent kinase 1, protein kinase B/Akt, mammalian target of rapamycin (mTOR), and p70 S6 kinase. Accordingly, the enhanced synthesis of fibrillin-1 was blocked by rapamycin, an inhibitor of mTOR. Notably, IGF-I, which signals through the same pathway, also stimulated fibrillin-1 synthesis. Systemic administration of rapamycin to mice subjected to unilateral ureteral obstruction, a model of renal fibrosis and increased fibrillin-1 synthesis, markedly reduced the number of interstitial fibroblasts and fibrillin-1 deposition. In streptozotocin-induced diabetes, IGF-I receptor was up-regulated in the kidneys from decorin-null mice. However, this could not compensate for the decorin deficiency, resulting ultimately in decreased fibrillin-1 content. This study provides evidence for the involvement of decorin and the IGF-I receptor/mTOR/p70 S6 kinase signaling pathway in the translational regulation of fibrillin-1. *(Am J Pathol 2007, 170:301–315; DOI: 10.2353/ajpath.2007.060497)*

Decorin (DCN) is the most thoroughly investigated member of the family of small leucine-rich proteoglycans, which are characterized by a core protein with centrally located leucine-rich motifs flanked by cysteine clusters and by glycosaminoglycan side chains covalently bound to the protein core. DCN carries a single chondroitin/dermatan-sulfate side chain at its N-terminal end (see review[1]). DCN was originally considered mainly to play a role in collagen fibril formation and stability (see review[2]), because ablation of the DCN gene is associated with disruption of type I collagen-containing fibrils, resulting in enhanced skin fragility in decorin-deficient mice.[3] DCN has additionally been shown to form complexes with transforming growth factor-β,[4] leading to inhibition and/or sequestration of this cytokine in the extracellular matrix.[5,6] Besides merely modulating cytokine activities, DCN is also directly involved in cell signaling, thereby regulating proliferation and apoptosis of various cell

Supported by the Deutsche Forschungsgemeinschaft (SFB 492, project B10 to L.S. and R.S.), the Interdisciplinary Center of Clinical Research, Münster (Schae2/026/06 to L.S. and R.S.), the Fund Innovative Medical Research of the University of Münster Medical School (SC 11 04 07 to L.S.), the Canadian Institutes of Health Research (MOP-68836 to D.P.R.), and the National Institutes of Health (CA39481 and CA47282 to R.V.I.).

This study is dedicated to the memory of Dr. Elke Schönherr, who passed away on August 7, 2005.

Accepted for publication October 12, 2006.

Address reprint requests to Liliana Schaefer, M.D., Pharmazentrum Frankfurt, Institut fur Allgemeine Pharmakologie und Toxikologie, Klinikum der JW Goethe-Universität Frankfurt am Main, Theodor-Stern-Kai 7, 60590 Frankfurt am Main, Germany. E-mail: schaefer@med.uni-frankfurt.de.

types *in vitro* and *in vivo* (see review[7]). In tumor cells, DCN binds to the epidermal growth factor receptor (EGFR) or ErbB4 and leads to activation of the mitogen-activated kinase pathway, to Ca^{2+} influx, to induction of the cyclin-dependent kinase inhibitor p21, and subsequently to down-regulation of the receptor.[8–10] In endothelial cells, DCN affects different pathways. It binds to the insulin-like growth factor-I receptor (IGF-IR) causing IGF-IR phosphorylation and activation,[11] resulting in enhanced phosphorylation of protein kinase B/Akt with subsequent induction of p21 by a mitogen-activated kinase-independent pathway.[12]

The IGF-IR, a ligand-activated protein tyrosine kinase, binds IGF-I and IGF-II (see review[13]) with high affinity. This interaction leads to autophosphorylation of the receptor and subsequent phosphorylation of downstream proteins, including insulin receptor substrate-1. In the next step, phosphoinositide 3-kinase (PI3K) is activated, increasing the level of phosphatidylinositol-3,4,5-trisphosphate. Phosphatidylinositol-3,4,5-trisphosphate co-recruits phosphoinositide-dependent kinase 1 (PDK1) and Akt to the membrane, resulting in phosphorylation of Akt and regulation of cell growth, apoptosis, and proliferation (see review[13]). Among the various downstream targets of the Akt signaling network, the mammalian target of rapamycin (mTOR) is responsible for the translational regulation exerted through p70 S6 kinase (p70 S6K) and ribosomal protein S6 (rp-S6) and the eukaryotic initiation factor 4B (eIF4B).[14] Akt signaling through direct phosphorylation of mTOR or inactivation of the tuberous sclerosis protein TSC2 leads to activation of mTOR. Conversely, rapamycin inhibits the activity of mTOR via binding to the FKBP12 component,[15,16] resulting, for example, in reduced synthesis of certain extracellular matrix proteins.[17,18] In addition, PDK1 can regulate translation independently of Akt by direct or protein kinase C (PKC) ζ-mediated phosphorylation of p70 S6K.[16,19]

Previously, we have shown in mesangial cells and renal fibroblasts as well as in an animal model of tubulointerstitial injury of the kidney [unilateral ureteral obstruction (UUO)] that DCN stimulates the synthesis of fibrillin-1.[20] Fibrillin-1 is the principal constituent of microfibrils, which in mature elastic fibers form a mantle around the elastic core or can be found as individual entities in nonelastic tissues. Mutations in the fibrillin-1 gene give rise to Marfan's syndrome, a heritable disease with severe aortic, ocular, and skeletal defects, and to a number of related connective tissue disorders generally termed type-1 fibrillinopathies. In individuals with Marfan's syndrome, down-regulation of DCN has been reported.[21,22] It is of note that DCN is capable of forming complexes with fibrillin-1.[23] At present, not much is known about the signaling pathways involved in the regulation of fibrillin-1. Angiotensin II and transforming growth factor-β have been shown to regulate fibrillin-1 expression in fibroblasts and mesangial cells.[24–26] In line with these findings, transforming growth factor-β antagonists and angiotensin II receptor blocker have recently been shown to prevent aortic aneurysms in a mouse model of Marfan's syndrome.[27] Interestingly, in bullous keratopathy stromal cells, both transforming growth factor-β and IGF-I modulate the synthesis of fibrillin-1.[28]

In this study, we established a molecular link between the DCN and IGF-I signaling pathways and the synthesis of fibrillin-1 in renal fibroblasts. Translational regulation of fibrillin-1 involved IGF-IR and the PI3K/Akt pathway with mTOR and p70 S6K as downstream targets. Importantly, in two animal models of renal tubulointerstitial injury and fibrosis, the enhanced deposition of fibrillin-1 was considerably reduced either due to the DCN deficiency, which could not be compensated for by enhanced expression of IGF-IR, or due to the administration of the mTOR inhibitor rapamycin.

Materials and Methods

Reagents

Hyperfilms, nitrocellulose membranes, radiochemicals, and the enhanced chemiluminescence reagents were acquired from GE Health Care Bio-Sciences (Freiburg, Germany). The BCA Protein Assay Reagent was purchased from Pierce (Rockford, IL). TRIzol, reagents for reverse transcriptase-polymerase chain reaction (RT-PCR), cell culture media, and sera were obtained from Invitrogen (Groningen, The Netherlands), and tissue culture plastic was from Falcon (Becton-Dickinson, Heidelberg, Germany). Antibodies used for Western blots were as follows: rabbit anti-human fibrillin-1,[29] rabbit-anti-human DCN,[30] rabbit anti-mouse DCN (LF-113),[31] and rabbit anti-human fibronectin (Sigma-Aldrich, Deisenhofen, Germany); mouse antibody to phosphotyrosine (clone PY20; Biomol, Hamburg, Germany); rabbit anti-β-chain of the IGF-IR (sc-713) and rabbit anti-β-tubulin (both from Santa Cruz Biotechnologies, Heidelberg, Germany); and anti-phospho-IGF-R (Tyr1131)/insulin receptor (Tyr1146), anti-phospho-PDK1 (Ser241), anti-PDK1, anti-phospho-PKCζ/λ (Thr410/403), anti-PKCζ, anti-phospho-Akt (Thr 308), anti-phospho-Akt (Ser473), anti-Akt, anti-phosphorylated Erk1/2 (Thr202/204), anti-total-Erk1/2, anti-phospho-mTOR (Ser2448), anti-mTOR, anti-phospho-p70 S6 kinase (Thr389), anti-p70 S6 kinase, anti-phospho-S6 ribosomal protein (Ser235/236), anti-S6 ribosomal protein, anti-phospho-eIF4B (Ser422), and anti-eIF4B (all raised in rabbits and all from Cell Signaling Technologies, Frankfurt/Main, Germany). As secondary antibodies, horseradish peroxidase-conjugated donkey anti-rabbit and sheep anti-mouse IgG were used for the correlating primary antibodies (GE Health Care Life Sciences). Tyrphostin AG1024 and AG1478 were obtained from Alexis (Grüneberg, Germany). Inhibitors of phosphoinositide 3-kinase (LY294002) and of MEK1/2 (U 0126) were from Cell Signaling Technologies. IGF-I and all other chemicals were purchased from Sigma-Aldrich.

Production and Purification of Decorin

Expression of human DCN and purification of the native proteoglycan were performed as described previously.[32]

In brief, for purification the conditioned medium was supplemented with proteinase inhibitors (0.1 mol/L ε-amino-*n*-caproic acid, 10 mmol/L ethylenediamine tetraacetic acid, 5 mmol/L benzamidine, 10 mmol/L *N*-ethylmaleimide, and 1 mmol/L phenylmethylsulfonyl fluoride) and applied to anion exchange chromatography on a DEAE-Trisacryl M column. DCN-containing eluate fractions were concentrated with Aquacide I according to the instructions of the manufacturer (Calbiochem, Schwalbach, Germany) and dialyzed for 2 hours against 20 mmol/L Tris-HCl, pH 7.4, containing 150 mmol/L NaCl. Final purification was achieved by high-performance liquid chromatography on a SEC-DEAE column (Phenomenex, Aschaffenburg, Germany) using a discontinuous NaCl gradient. The purity of DCN for all experiments was checked by sodium dodecyl sulfate (SDS)-polyacrylamide gel electrophoresis and silver staining. For some experiments, the proteoglycan was digested with chondroitinase ABC (Seikagaku Kogyo, Tokyo, Japan) to remove chondroitin sulfate and dermatan sulfate chains or was conjugated with digoxigenin.[33]

Cell Culture and Stimulation

Normal rat kidney (NRK) fibroblasts (American Type Culture Collection, Rockville, MD) were cultured as described previously.[20] To obtain quiescent NRK fibroblasts, cells were maintained in serum-free Dulbecco's modified Eagle's medium supplemented with 0.1 mg/ml fatty acid-free bovine serum albumin for 24 hours before the addition of recombinant human DCN and IGF-I. Because NRK cells display concentration-dependent responses at concentrations between 1 and 10 μg/ml recombinant proteoglycans and 10 and 200 ng/ml IGF-I (unpublished data), we used 4 μg/ml DCN and 100 ng/ml IGF-I for all further experiments. Intact proteoglycans were used in the majority of experiments because this is their presumed natural form *in vivo*. When required, NRK cells were preincubated for 30 minutes with tyrphostin AG1024 and AG1478 (both 10 μmol/L) or for 1 hour with the inhibitor of phosphoinositide 3-kinase LY294002 (50 μmol/L) and with 10 μmol/L MEK1/2 inhibitor, respectively. Viability of cells was not altered under these conditions, as determined by lactate dehydrogenase release into the culture supernatant using a cytotoxicity detection kit (Roche Applied Science, Mannheim, Germany).

Western Blot Analysis

Western blots were performed and quantified as described previously.[6] Protein bands were visualized using the enhanced chemiluminescence Western blotting reagent kit and quantified with IQ Solutions Image Quant software (Molecular Dynamics, Uppsala, Sweden). Results from kidney samples are expressed as optical density normalized by β-tubulin. Data from culture supernatants or from cell homogenates were normalized by cell number, by total protein content, by β-tubulin, or by corresponding nonphosphorylated proteins in homogenized cells. For quantification, the results of three samples per group were averaged.

Immunoprecipitation

The IGF-I receptor from NRK cells was immunoprecipitated with the antibody sc-713 as described previously[11] with some modifications. NRK cells (10^7) were incubated with 8 μg of intact human DCN or 400 ng of IGF-I for 2 hours at 4°C followed by incubation with 1 mmol/L 3,3′-dithiobis(sulfosuccinmidylpropionate), a thiol-cleavable, primary amino-reactive cross-linker (Pierce) used for cross-linking of DCN or IGF-I with cell surface proteins. Cells were harvested in lysis buffer (10 mmol/L sodium phosphate, pH 7.5, 150 mmol/L NaCl, 1% Triton X-100, 0.5% sodium deoxycholate, 0.1% SDS, 2 mmol/L sodium vanadate, and proteinase inhibitors), and cell lysates were incubated for 6 hours with a complex of normal rabbit serum bound to protein A-Sepharose (Sigma) to remove nonspecifically binding proteins. Then, 10 μg of the rabbit anti-IGF-IR was added, and after 16 hours, immune complexes were precipitated with protein A-Sepharose. As control, the same amount of protein A-Sepharose was incubated with the antibody in the absence of cell lysates. Additional controls included samples incubated without cross-linker and/or without DCN and IGF-I, respectively. After washing (3× lysis buffer and 2× phosphate-buffered saline), the material was divided into two aliquots, and one aliquot was digested with chondroitinase ABC to allow for identification of the decorin core protein. Bound proteins were eluted by boiling in sample buffer for 5 minutes. Subsequently, samples were analyzed by Western blotting for the presence of DCN and IGF-IR.

To examine phosphorylation of IGF-IR, NRK cells were incubated either with DCN (4 μg/ml) or with IGF-I (100 ng/ml) for 5 minutes and subsequently immunoprecipitated for IGF-IR followed by Western blot using an antibody that recognizes phosphotyrosine residues. The same blot was reprobed with the antibody to IGF-IR. Quantification of IGF-IR phosphorylation was performed as described above and was normalized to IGF-IR.

Binding of DCN to IGF-IR

To determine binding of DCN to the IGF-IR, the receptor was immunoprecipitated from NRK cells (7×10^6 cells) with the antibody sc-713. Cells were harvested in lysis buffer, and a complex of normal rabbit serum bound to protein A-Sepharose was added for 6 hours to remove nonspecifically bound proteins. Then 10 μg of the anti-IGF-IR was added, and after 16 hours, the antibodies were precipitated with protein A-Sepharose. As control, a similar amount of protein A-Sepharose was incubated with the antibody but without cell lysate. After washing (3× lysis buffer and 2× phosphate-buffered saline), the material was divided into five aliquots and incubated in 250 μl of Tris-buffered saline, 0.1% bovine serum albumin, and 0.1% Tween 20 with [^{35}S]sulfate-labeled DCN or human recombinant 3-[^{125}I]iodotyrosyl IGF-I (GE Health

Care Bio-Sciences) at 4°C overnight. Preparation and purification of [^{35}S]sulfate DCN from human skin fibroblasts was described previously.[34] DCN had a molar activity of 5.4×10^{15} cpm/mol and IGF-I of 5.0×10^{17} cpm/mol. For inhibition experiments, unlabeled wild-type DCN was added to bound-labeled IGF-I. After washing four times with binding buffer, bound proteins were removed by boiling in 1% SDS, and ligands bound to the receptor were quantified by scintillation counting and correlating the amount of [^{35}S]sulfate or ^{125}I to the protein concentration of DCN or IGF-I, respectively. Nonspecific binding values, measured in immune complexes without the receptor, were subtracted from sample values to obtain specific DCN- or IGF-I-binding signals. The concentration of radioligands added was very similar to the concentration of free radioligands in solution. Dissociation constants were determined with GraphPad, Prism4 software using the subroutine for fitting one-site binding curves (GraphPad Software, San Diego, CA).

Animal Experiments

All animal experimentation was conducted in accordance with the German Animal Protection Act and was approved by the ethics review committee for laboratory animals of the District Government of Muenster (Muenster, Germany). Obstruction of the left ureter (unilateral ureteral obstruction) was performed in 2-month-old male C57BL/6 mice.[35] The contralateral kidney served as control. Mice were divided into two groups: UUO mice and UUO mice treated with rapamycin. Rapamycin (1.8 mg kg^{-1} day^{-1}) or vehicle was intraperitoneally administered daily to control and UUO mice. Kidneys ($n = 8$ per group) were analyzed at day 7 after renal obstruction.

Type 1 diabetes mellitus was induced in 2-month-old male $Dcn^{-/-}$ and $Dcn^{+/+}$ mice by three consecutive daily intraperitoneal injections of streptozotocin (STZ; Sigma-Aldrich) (45 mg/kg body weight) dissolved in 100 mmol/L sodium citrate buffer (pH 4.5). Control animals were injected only with citrate buffer. Mice with glucosuria were implanted with a subcutaneous insulin pellet (Linplant; Linshin, Ontario, ON, Canada) to prevent ketoacidosis. Blood glucose was controlled every 10 days (Haemo-Glukotest; Roche Diagnostics, Mannheim, Germany). Urine glucose and ketone bodies were measured with urinalysis reagent strips (Keto-Diastix; Bayer Vital, Leverkusen, Germany). Urinary protein and creatinine excretion was determined with the BCA Protein Assay Reagent and Creatinine Assay kit (NatuTec, Frankfurt/Main, Germany). Kidneys ($n = 6$ per group) were analyzed 9 weeks after induction of diabetes.

Morphological and Immunohistochemical Studies

Serial sections (4 μm) of paraffin-embedded samples were either stained with periodic acid-Schiff reaction, modified Masson trichrome stain[36] or processed for immunohistochemical studies by immunoperoxidase or alkaline phosphatase anti-alkaline phosphatase techniques.[35] Primary antibodies included rabbit anti-human fibrillin-1,[29] which extensively cross-reacts with mouse fibrillin-1, rabbit anti-murine DCN (LF-113),[31] rabbit anti-S100A4 (marker of fibroblast-like cells; DakoCytomation, Glostrup, Denmark), rabbit anti-IGF-IR (sc-713), rabbit anti-rat collagen type I (Quartett Immunodiagnostika und Biotechnologie, Berlin, Germany), rabbit anti-human fibronectin (Sigma-Aldrich), and anti-Ki-67 (marker of cell proliferation; Dianova, Hamburg, Germany). Apoptosis was assayed by TUNEL staining (Roche Applied Science) as described previously.[35] Counterstaining was with methyl green or with Mayer's hemalaun. The specificity of immunostaining was ascertained using negative controls by omitting the primary antibody and using nonimmune serum.

To evaluate individual kidneys, 15 randomly selected nonoverlapping fields of renal cortex were examined under ×400 magnification, and the number of S100A4-positive fibroblasts, Ki-67-positive nuclei, and apoptotic nuclei were evaluated. Staining for S100A4 was found in spindle-shaped interstitial cells and also in cells that were round, probably representing inflammatory cells. Only spindle-shaped cells were included in the counts. Morphometrical evaluation of collagen type I and fibronectin or collagenous connective tissue stained with a modified Masson trichrome technique (green color) was performed using cell imaging software (Soft Imaging System; Olympus, Tokyo, Japan). Sections were examined by a blinded observer. Mean values of at least three kidneys per group were averaged.

Immunostaining for fibrillin-1 and for fibroblast-like cells (S100A4) was performed on serial sections from untreated, ligated kidneys as described previously.[37] This method was preferred over double immunostaining, because both primary antibodies were available only in hosts of the same origin (rabbit). Alexa Fluor 488 donkey anti-rabbit IgG (Invitrogen) and Cy3-conjugated donkey anti-rabbit IgG (Dianova, Hamburg, Germany) were used for visualization of fibrillin-1 and S100A4, respectively. Nuclear staining was performed with Draq5 (Alexis). Nonspecific staining was determined by the use of secondary antibodies alone.

Northern Blot Analysis

Total RNA was extracted as described previously.[6] To generate the probe specific for rat fibrillin-1, cDNA was prepared by reverse transcription of total RNA from rat kidney using oligo dT primer and Superscript II as instructed by the manufacturer (Invitrogen). The cDNA was amplified by the polymerase chain reaction with oligo nucleotides 5′-GCTCAAGACCAAACATGTGC-3′ and 5′-CAATTTCCTCCTTGACACAG-3′, resulting in a 504-bp fragment (nucleotides 281 to 785). The amplified DNA fragment was cloned into the pCR II vector (Invitrogen). The cDNA probe for glyceraldehyde-3-phosphate dehydrogenase was from American Type Culture Collection. Northern blots were performed and analyzed as described previously.[6] The murine cDNAs for fibrillin-1 and glyceraldehyde-3-phosphate dehydrogenase were described previously.[20] Quantification was performed with a STORM860 PhosphorImager using IQ Solutions Image

Quant software (both from Molecular Dynamics). Each individual mRNA band was normalized to glyceraldehyde-3-phosphate dehydrogenase to correct for differences in RNA loading and/or transfer. Values are given as means ± SEM from three Northern blots.

Determination of Decorin and Collagen Type I in Kidney Homogenates

DCN in homogenates from whole contralateral and ligated kidneys ($n = 3$ in each group) was extracted, semipurified, and quantified as described previously.[6,33] In brief, kidney homogenates and appropriate standard solutions were supplemented with 10 mmol/L Tris/HCl, pH 7.4, 0.1% Triton X-100, and protease inhibitors. Subsequently, samples were mixed with DEAE Trisacryl M (100 mg wet weight; Serva, Heidelberg, Germany) preequilibrated with 20 mmol/L Tris/HCl, pH 7.4, containing 0.15 mol/L NaCl, 0.1% Triton X-100, and protease inhibitors (buffer 1) and mixed by rotation for 1 hour at 4°C. The samples were washed sequentially with 3 ml of buffer 1 containing in addition 7 mol/L urea, 3 ml of urea-free buffer 1, and 3 ml of buffer 1 containing 0.3 mol/L NaCl instead of 0.15 mol/L NaCl. Elution was achieved with 1.5 ml of buffer 1 containing 1 mol/L NaCl instead of 0.15 mol/L NaCl. On the addition of 5 vol of methanol and 1 vol of chloroform to the eluates, proteoglycans were collected at the interphase between chloroform and aqueous methanol and washed with methanol. The proteoglycans were then digested with chondroitinase ABC to remove glycosaminoglycan chains and subjected to polyacrylamide gel electrophoresis followed by Western blotting with subsequent quantification.

Collagen type I was determined after exhaustive pepsin digestion of whole minced contralateral and ligated kidneys followed by 4 to 12.5% SDS-polyacrylamide gel electrophoresis under reducing and nonreducing conditions and quantification (IQ Solutions Image Quant software) of Coomassie Blue-stained bands of α1(I)- and α2(I)-chains of collagen I. Pepsin-digested purified type I, III, and IV collagens were used as standards (kindly provided by J. Rauterberg, University of Münster, Münster, Germany). For Western blotting and type I collagen quantification, the results from three kidneys per group were averaged.

Statistics

Data are given as means ± SEM analyzed by one-way analysis of variance, with Dunnett's significance correction test (SPSS software; SPSS Inc., Chicago, IL). Differences were considered significant at P values <0.05.

Results

Decorin Induces Fibrillin-1 Protein Expression in NRK Cells via IGF-IR

We exposed NRK cells to human recombinant DCN (4 μg/ml, ~40 nmol/L)[20] or IGF-I (100 ng/ml, 12.5 nmol/L)[28] for 6 hours (Figure 1, A and B) and 24 hours (data not shown) in the presence or absence of specific inhibitors of the IGF-IR or EGFR.[38] Quantification of Western blots for fibrillin-1 in the NRK cell culture supernatants confirmed the stimulatory effect of DCN (2.8- ± 0.6-fold increase) and provided additional evidence for a similar effect of IGF-I (1.9- ± 0.5-fold increase) (both $n = 3$, $P < 0.05$; 6 hours; normalized to β-tubulin in cell homogenates), because both seemed to be strong inducers of fibrillin-1 secretion from renal fibroblasts (Figure 1, A and B). Comparable results were obtained when the amount of fibrillin-1 was normalized to the total protein content of the cells, to β-tubulin in cell homogenates, or to the number of cells. Moreover, pre-incubation with tyrphostin AG1024 (10 μmol/L), an inhibitor of the IGF-IR tyrosine kinase, prevented the DCN- and IGF-I-induced increments in fibrillin-1 secretion and completely abolished baseline synthesis (probably caused by endogenous IGF-I or DCN) of fibrillin-1 in NRK cells (Figure 1A). In contrast, the EGF receptor inhibitor tyrphostin AG1478 (10 μmol/L) had no effect on DCN- or IGF-I-induced secretion of fibrillin-1 from NRK cells (Figure 1B). Even though fibrillin-1 is primarily a secreted protein, an increase in fibrillin-1 content could also be detected in the homogenates of NRK cells on incubation with DCN and IGF-I, albeit to a lesser extent than what was found in the supernatants (data not shown). The increase in fibrillin-1 in cell homogenates was also sensitive to inhibition by AG1024. This clearly suggests that the larger quantities of fibrillin-1 found in the culture supernatants after incubation with DCN or IGF-I were in fact due to higher synthesis of fibrillin-1. In addition, Northern blots of NRK cells cultured for 2 hours[20] with or without AG1024 did not show any decline in fibrillin-1 mRNA, indicating that IGF-IR-dependent regulation of fibrillin-1 synthesis does not occur at the transcriptional level (DCN, 1.6 ± 0.4; IGF-I, 1.8 ± 0.5; DCN + AG1024, 1.8 ± 0.6; IGF-I + AG1024, 1.7 ± 0.6; $n = 3$, $P > 0.05$, Northern blots of fibrillin-1 mRNA normalized to glyceraldehyde-3-phosphate dehydrogenase).

The binding properties of DCN and IGF-I to the isolated IGF-IR from NRK cells were investigated using [^{35}S]sulfate-labeled DCN and 3-[^{125}I](iodotyrosyl) IGF-I. This method was preferred over direct binding of DCN to IGF-IR on the cell surface of NRK cells, because interaction of DCN with other cell surface molecules cannot be excluded. Therefore, the IGF-IR was immunoprecipitated with antibody against its intracellular domain (β-subunit) and incubated with radiolabeled DCN and IGF-I. These binding assays revealed strong binding in the low nanomolar range for IGF-I ($K_D = 0.4 \times 10^{-9}$ mol/L) and for DCN ($K_D = 8.1 \times 10^{-9}$ mol/L) to IGF-IR (Figure 1, C and D). In a further experiment, ^{125}I-IGF-I was bound to the receptor and then displaced by unlabeled DCN. DCN inhibited IGF-I-binding to the IGF-IR with an estimated IC_{50} of 3×10^{-8} mol/L (Figure 1E).

In addition, we found that DCN directly added to NRK cells co-immunoprecipitated with IGF-IR (Figure 1F). Importantly, immunoprecipitation of the IGF-IR on NRK cells, which had been stimulated with DCN or IGF-I for 5 minutes, followed by Western blotting using an antibody

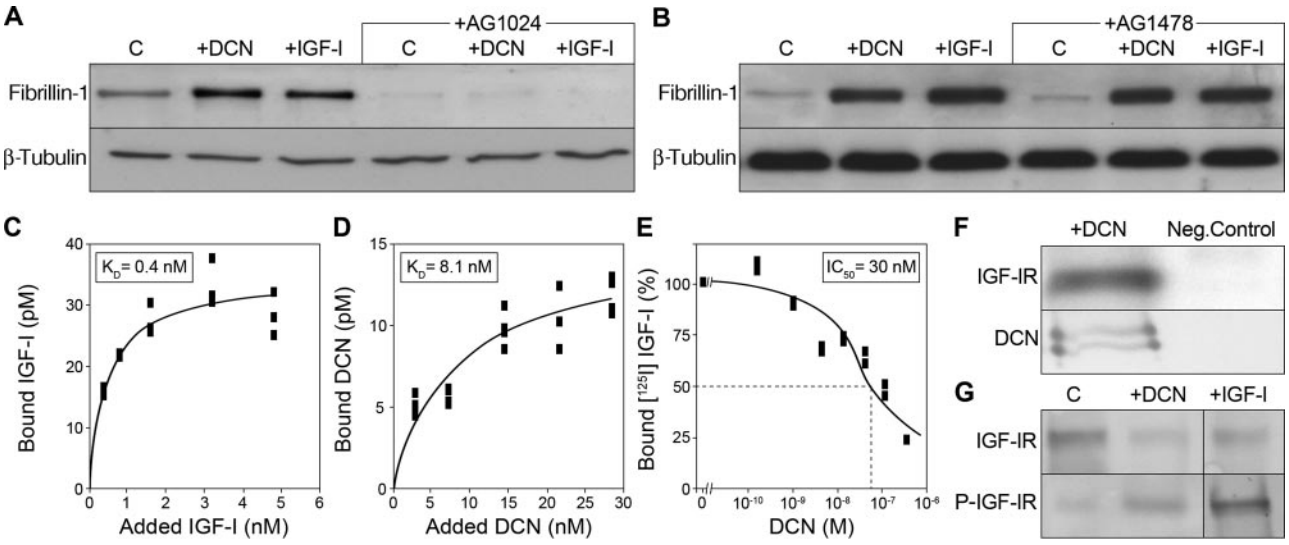

Figure 1. Decorin and IGF-I induce fibrillin-1 protein synthesis in normal rat kidney fibroblasts via the IGF-IR. **A** and **B** show representative Western blots for fibrillin-1 in culture supernatants from NRK cells incubated for 6 hours with recombinant DCN or IGF-I in the presence or absence of tyrphostin AG1024 (**A**) (inhibitor of the IGF-IR tyrosine kinase) or AG1478 (**B**) (inhibitor of the EGFR tyrosine kinase). β-Tubulin in the homogenates of NRK cells is shown as control. Only the IGF-IR inhibitor (**A**) but not the EGFR inhibitor (**B**) blocked DCN- or IGF-I-mediated secretion of fibrillin-1 from NRK cells. **C–E:** IGF-IR was immunoprecipitated from NRK cells. Each data point represents immune complexes with the receptor from 1×10^6 cells. **C:** Binding curve of ^{125}I-IGF-I. **D:** Binding curve of [^{35}S]sulfate-labeled DCN. **E:** In inhibition experiments, IGF-I receptor immunoprecipitated from NRK cells was incubated with 400 pmol/L ^{125}I-IGF-I in the presence or absence of the indicated amounts of unlabeled DCN. The dashed line indicates estimated 50% inhibition. **F:** Co-immunoprecipitation of IGF-IR and DCN after incubation of NRK cells with DCN, followed by Western blot analysis for IGF-IR (**top**) and DCN core protein (after chondroitinase ABC treatment; **bottom**). Negative control represents protein A-Sepharose incubated with antibody but without cell lysate. **G:** NRK cells were incubated with DCN or IGF-I for 5 minutes. Immunoprecipitations for the IGF-IR were followed by Western blots probed for phosphotyrosine residues (P-IGF-IR; **bottom**) and reprobed for IGF-RI itself (**top**).

that recognizes phosphotyrosine residues showed that IGF-IR is phosphorylated in response to both DCN and IGF-I (Figure 1G). After normalization to the amount of IGF-IR, DCN increased receptor phosphorylation 8.7 ± 1.8-fold and IGF-I 11.6 ± 2.6-fold (both $n = 3$, $P < 0.05$). Reprobing the same blots with an antibody to phospho-IGF-R (Tyr1131) indicated that the receptor tyrosine kinase was in fact active (not shown).

Decorin-Mediated Regulation of Fibrillin-1 Protein Expression in NRK Cells Involves the PI3K/Akt Pathway

The involvement of the IGF-IR signaling system in the regulation of fibrillin-1 protein synthesis was characterized in NRK cells. The role of PI3K in the regulation of fibrillin-1 was investigated by incubating NRK cells with DCN or IGF-I for 6 hours in the presence and absence of LY294002, a PI3K inhibitor. LY294002 in a final concentration of 50 μmol/L almost completely blocked DCN- and IGF-I-triggered secretion of fibrillin-1 protein into NRK culture supernatants (Figure 2A) and intracellular synthesis (data from homogenates not shown), without acting as a general inhibitor of protein synthesis (as evidenced by measurements of total protein and β-tubulin in NRK cell homogenates; Figure 2A, bottom). LY294002 had no influence on fibrillin-1 mRNA (not shown), indicating again that transcriptional regulation of fibrillin-1 was not involved. Further analysis of the downstream signaling of PI3K showed enhanced phosphorylation of the PDK1 6 minutes after incubation of NRK cells with DCN (3.4 ± 0.8-fold increase) or IGF-I (2.7 ± 0.7-fold increase, both $n = 3$, $P < 0.05$) (Figure 2B). In addition, time-course experiments (5 to 15 minutes) revealed maximal induction of Akt/PKB phosphorylation at Ser473 and Thr308 after 8 minutes of incubation of NRK cells with DCN or IGF-I (DCN, 2.4 ± 0.7 times control; IGF-I, 2.9 ± 0.8-fold increase, both $n = 3$, $P < 0.05$) (Figure 2, C and D). These stimulatory effects were blocked by incubation with inhibitors of IGF-IR (Figure 2C) and PI3K, respectively (Figure 2D).

Incubation of NRK cells (5 to 60 minutes) with DCN or IGF-I had no influence on the phosphorylation of Erk1/2 (Figure 2E). In agreement with these findings, the inhibitor of MEK1/2 (U 0126) had no effect on DCN- or IGF-I-mediated synthesis of fibrillin-1 in NRK cells (data not shown), indicating that the mitogen-activated kinase pathway is not involved in this process. In addition, phosphorylation of PKCζ after incubation of NRK cells with DCN or IGF-I was excluded, suggesting that neither DCN nor IGF-I stimulate PKCζ downstream of PDK1 (Figure 2F).

DCN- and IGF-I-Dependent Regulation of Fibrillin-1 in NRK Cells Involves mTOR and p70 S6K Downstream of Akt

Next, we examined the influence of DCN and IGF-I on mTOR, a downstream mediator of Akt responsible for translational regulation and its potential involvement in the regulation of fibrillin-1 synthesis in NRK cells. In fact, incubation of NRK cells with DCN (2.3 ± 0.5-fold increase) or IGF-I (2.1 ± 0.3-fold increase; both $n = 3$, $P < 0.05$) for 8 minutes resulted in enhanced mTOR phos-

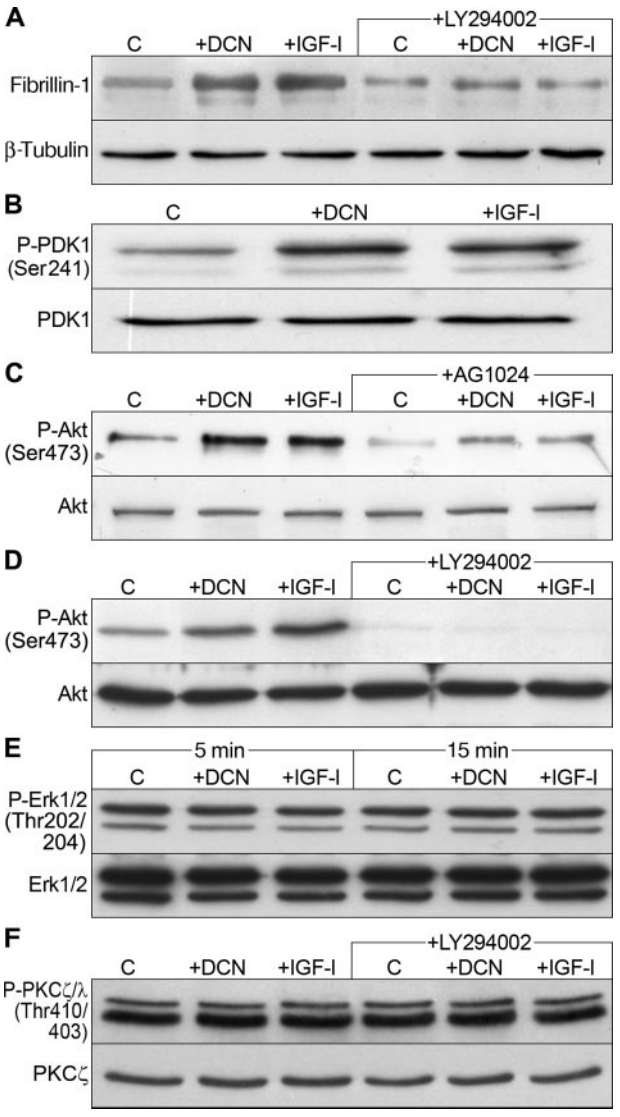

Figure 2. Involvement of the PI3K/Akt pathway in DCN- and IGF-I-mediated regulation of fibrillin-1 in NRK cells. **A:** Western blot for fibrillin-1 in culture supernatants from NRK cells incubated for 6 hours with recombinant DCN or IGF-I in the presence or absence of LY294002 (inhibitor of PI3K). β-Tubulin in NRK cell homogenates is shown as control. **B:** Phosphorylation of PDK1 in NRK cells after 6 minutes of incubation with DCN or IGF-I (Western blot). **C** and **D:** phosphorylation of Akt in NRK cells after 8 minutes of incubation with DCN or IGF-I (Western blots) was blocked by inhibition of IGF-IR (AG1024) (**C**) or by inhibition of PI3K (LY294002) (**D**). **E** and **F:** DCN and IGF-I had no influence on the phosphorylation of Erk1/2 (**E**) or of PKCζ (**F**) in NRK cells (Western blot).

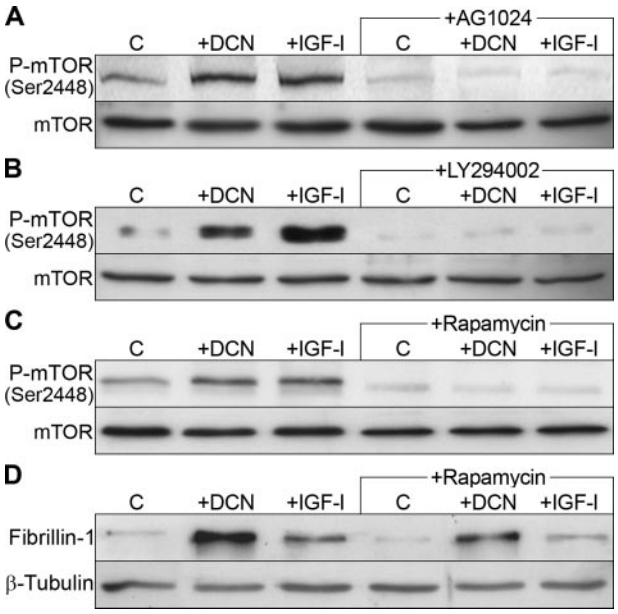

Figure 3. DCN- and IGF-I-dependent regulation of fibrillin-1 in NRK cells involves mTOR. **A–C:** DCN- and IGF-I-mediated phosphorylation of mTOR in NRK cells (8 minutes of incubation) was suppressed by inhibition of IGF-IR (**A**), by an inhibition of PI3K (**B**), and by rapamycin (inhibitor of mTOR) (**C**) (Western blots). **D:** Western blot for fibrillin-1 in culture supernatants of NRK cells incubated for 6 hours with recombinant DCN or IGF-I in the presence or absence of rapamycin. β-Tubulin in the NRK cell homogenates is shown as control. Rapamycin only partially inhibited DCN- or IGF-I-mediated secretion of fibrillin-1 from NRK cells.

phorylation at Ser2448 (Figure 3, A–C). Phosphorylation was inhibited by AG1024 (Figure 3A), LY294002 (Figure 3B), and rapamycin (Figure 3C), indicating involvement of IGF-IR and PI3K in DCN- and IGF-I-mediated activation of mTOR. Furthermore, incubation of NRK cells with rapamycin for 6 hours inhibited the DCN-mediated (69 ± 18% of control; $n = 3$, $P < 0.05$) and IGF-I-mediated (58 ± 16% of control; $n = 3$, $P < 0.05$) increase in fibrillin-1 synthesis (Figure 3D), demonstrating that mTOR is involved in the translational regulation of fibrillin-1 downstream of PI3K. In addition, Northern blots of NRK cells incubated with rapamycin did not show any down-regulation of fibrillin-1 mRNA, indicating that mTOR-dependent regulation of fibrillin-1 does not occur at a transcriptional level (data not shown).

Because mTOR exerts its influence as a translational regulator through p70 S6K,[39] we investigated the influence of DCN or IGF-I on the activation of p70 S6K. Phosphorylation of p70 S6K at Thr389 was induced after 8 minutes of incubation with DCN (1.7 ± 0.4-fold increase; $n = 3$, $P < 0.05$) or IGF-I (2.2 ± 0.4-fold increase; $n = 3$, $P < 0.05$) (Figure 4, A–C). As expected, AG1024 (Figure 4A) and LY294002 (Figure 4B) abolished DCN- and IGF-I-dependent activation of p70 S6K. In contrast, rapamycin only partially inhibited the stimulatory effects of DCN (32 ± 7%, $n = 3$, $P < 0.05$) and of IGF-I (41 ± 11%, $n = 3$, $P < 0.05$) on p70 S6K (Figure 4C), indicating that p70 S6K stimulation by DCN and IGF-I is only in part mediated through mTOR. Moreover, downstream to p70 S6K, both the rp-S6 and eIF4B were phosphorylated by DCN (rp-S6, 1.8 ± 0.4-fold increase; eIF4B, 1.9 ± 0.3-fold increase; $n = 3$, $P < 0.05$) or IGF-I (rp-S6, 1.7 ± 0.3-fold increase; eIF4B, 1.8 ± 0.4-fold increase; $n = 3$, $P < 0.05$) at Ser235/236 and Ser422, respectively, and these effects were abolished by AG1024 (Figure 4, D and E).

In Vivo *Decorin-Mediated Regulation of Fibrillin-1*

To test whether the *in vitro* findings reported above might have biological relevance in an *in vivo* setting, we used an established animal model of UUO. This model leads to a pronounced interstitial inflammation and fibrosis and a

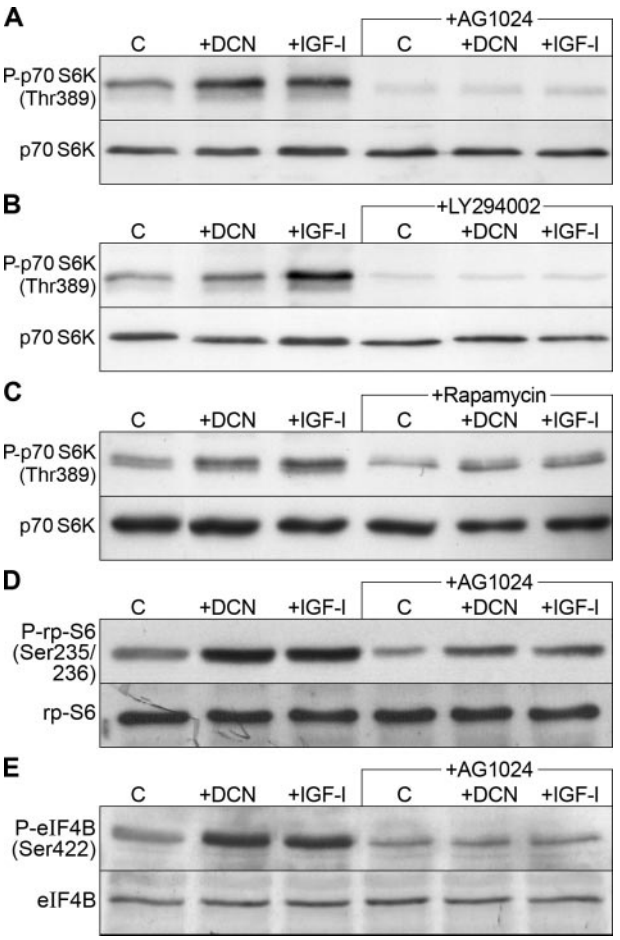

Figure 4. DCN and IGF-I lead to increased phosphorylation of p70 S6K, rpS6, and eIF4B downstream of mTOR. **A–C:** DCN- and IGF-I-mediated phosphorylation of p70 S6K in NRK cells (8 minutes of incubation) was suppressed by inhibition of IGF-IR (**A**) and by an inhibition of PI3K (**B**). The mTOR inhibitor (**C**) only partially blocked DCN- or IGF-I-mediated phosphorylation of p70 S6K (Western blots). **D** and **E:** DCN- and IGF-I-mediated phosphorylation of rp-S6 (**D**) and eIF4B (**E**) in NRK cells (8 minutes of incubation) was suppressed by inhibition of the IGF-IR tyrosine kinase.

concurrent induction of fibrillin-1 synthesis in the ligated kidney.[20] Rapamycin (1.8 mg kg^{-1} day^{-1}) or vehicle was administered intraperitoneally to UUO mice. At day 7, severe hydronephrosis had developed both in rapamycin-treated and untreated animals. However, obstructed kidneys from rapamycin-treated mice were smaller in both size and weight. After aspiration of urine from the dilated pyelon, the weight of kidneys from rapamycin-treated animals was 119 ± 9 versus 159 ± 8 mg in untreated animals ($n = 8$; $P < 0.05$). No differences were observed in body weight or in the weight of the contralateral kidneys between both groups. Light microscopy of periodic acid-Schiff-stained sections showed that tubuli were slightly more dilated in ligated kidneys from rapamycin-treated compared with control mice (Figure 5A). Contralateral kidneys from rapamycin-treated and untreated animals were similar in terms of renal morphology (Figure 5A). As expected, UUO caused enhanced proliferation of tubular epithelial cells and peritubular interstitial cells.[35,40] Treatment with rapamycin markedly reduced proliferation of tubular epithelial cells in ligated kidneys (Figure 5, B and C). A similar effect could also be observed in contralateral kidneys, albeit at generally lower proliferation rates (Figure 5C). In addition, reduced numbers of Ki-67-positive peritubular interstitial cells were detected in ligated kidneys after treatment with rapamycin (Figure 5C). Rapamycin had no effect on apoptosis of tubular epithelial cells and peritubular interstitial cells in obstructed and contralateral kidneys (data not shown).

To examine whether treatment with rapamycin would impact on the renal expression of fibrillin-1, proteins were extracted from whole-kidney homogenates, and fibrillin-1 was quantitated by Western blot analysis. There was an increase in fibrillin-1 protein in the ligated compared with contralateral kidneys from both rapamycin-treated and control mice at day 7 (Figure 6A). This was due to a pronounced accumulation of fibrillin-1 in the peritubular areas, in tubular basement membranes, and in Bowman's capsule (Figure 6D). However, in ligated kidneys from rapamycin-treated mice, there was a significant (more than 1.6-fold) reduction of fibrillin-1 protein deposition compared with ligated kidneys from untreated animals (Figure 6, A and B). These quantitative data were further confirmed by immunostaining for fibrillin-1 in tissue sections from ligated kidneys, where a lower intensity of staining was found predominantly in the peritubular areas in rapamycin-treated kidneys (Figure 6D). In agreement with the data indicating lower number of proliferating peritubular cells, quantification of interstitial fibroblast-like cells (S100A4-positive) revealed a reduction in cell number in ligated kidneys treated with rapamycin compared with untreated kidneys [rapamycin, 73 ± 4.1, versus control, 90 ± 5.6; $n = 5$; $P < 0.05$, S100A4-positive cells/high-power field, quantified in 20 fields (×400) per section]. Staining for S100A4 was found in spindle-shaped interstitial cells and also in cells that were round, probably representing inflammatory cells. Only spindle-shaped cells were included in the counts. Immunostaining for fibrillin-1 and S100A4 on two serial sections from untreated, ligated kidneys indicated a close spatial proximity of fibrillin-1 to fibroblast-like cells (Figure 6E), suggesting that the reduced deposition of fibrillin-1 in rapamycin-treated, ligated kidneys is apparently due to both a lower number of fibrillin-1-producing fibroblasts and decreased fibrillin-1 production by fibroblasts treated with rapamycin.

To explore whether these rapamycin effects on fibrillin-1 were due to a general inhibition of protein synthesis, we also quantified fibronectin deposition in ligated kidneys from rapamycin-treated and control mice. As expected, expression of fibronectin protein was also enhanced in ligated compared with contralateral kidneys (Figure 6A). However, the administration of rapamycin had no effect on the amount of fibronectin deposited in the kidneys (Figure 6, A and C). By contrast, the deposition of collagen was markedly reduced in ligated kidneys after administration of rapamycin, as evidenced by Masson trichrome staining (Figure 6, F and G). In agreement with these data, deposition of type I collagen, assessed by quantification of extractable collagens by SDS-polyacrylamide gel electrophoresis and densitome-

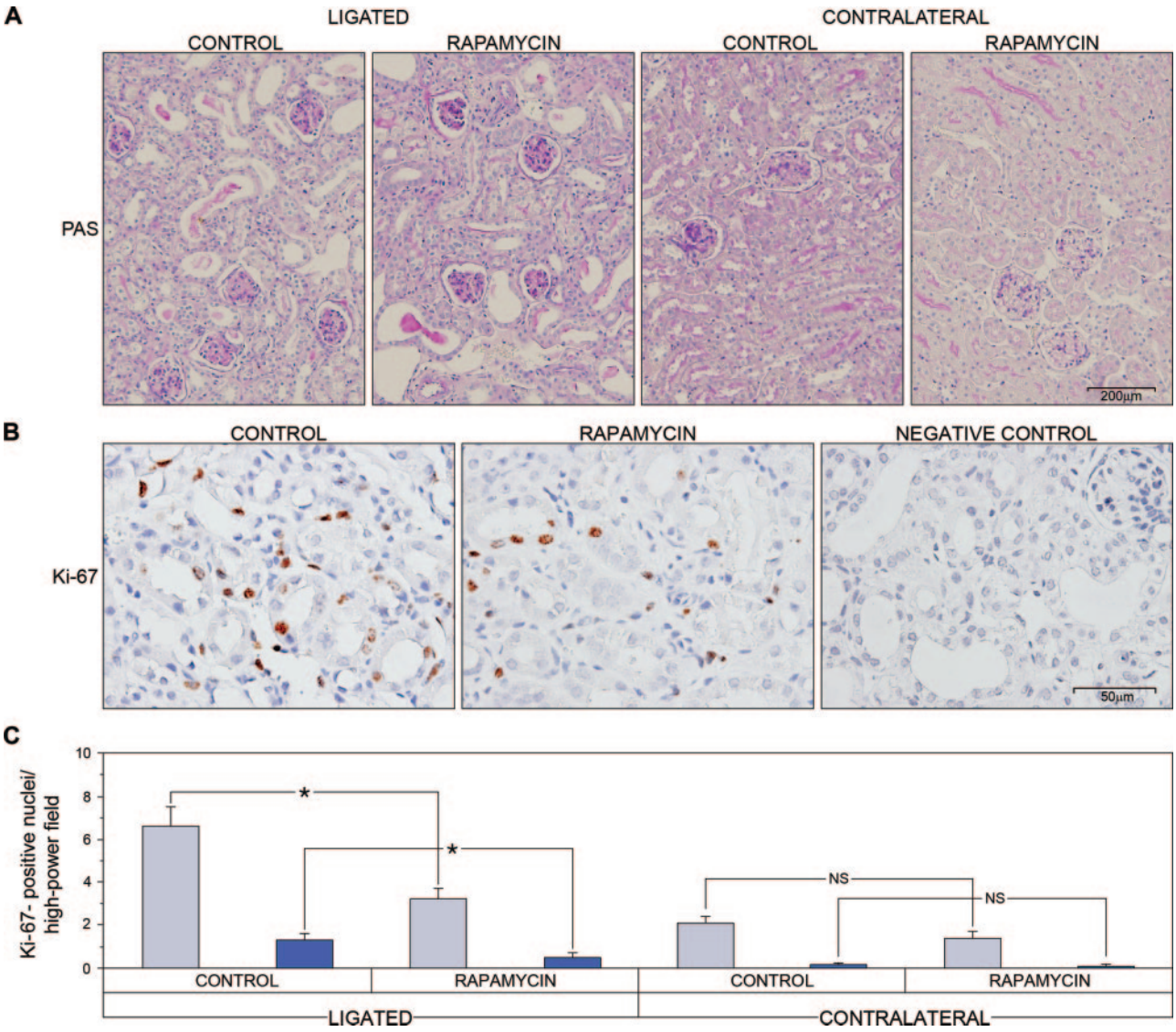

Figure 5. In vivo effects of rapamycin on proliferation of tubular epithelial and peritubular cells 7 days after UUO. **A:** Periodic acid-Schiff (PAS)-stained sections from ligated and contralateral kidneys from control and rapamycin-treated mice 7 days after UUO. **B:** Immunostaining of proliferating tubular epithelial and peritubular cells in ligated kidneys from control and rapamycin-treated mice (Ki-67-positive nuclei, peroxidase, brown). Counterstaining was with methyl green. Scale bars: 200 μm (**A**) and 50 μm (**B**). **C:** Quantification of Ki-67-positive nuclei in tubular epithelial cells/high-power field (blue bars) and in peritubular cells/high-power field (navy blue bars) in control and rapamycin-treated kidneys [quantified in 20 fields (magnification, ×400) per section]. The **asterisk** indicates statistical significance; $n = 4$, $P < 0.05$.

try [sum of α1(I)- and α2(I)-chains], was lower (2.2 ± 0.4-fold reduction, $n = 3$, $P < 0.05$) in obstructed kidneys from rapamycin-treated mice (Figure 6H).

Western blot analysis of semipurified proteoglycans from ligated and contralateral kidneys, digested with chondroitin ABC lyase to remove glycosaminoglycan chains, demonstrated enhanced accumulation of DCN in ligated kidneys (Figure 7A). Unlike the results obtained for fibrillin-1, deposition of DCN was particularly pronounced after administration of rapamycin (Figure 7A). This observation was further confirmed by immunohistochemistry, demonstrating that in ligated kidneys from rapamycin-treated mice, more DCN protein was present primarily in the perivascular and peritubular space (Figure 7B). Differences between contralateral kidneys from rapamycin-treated and untreated animals were not observed.

The implication that DCN-mediated regulation of fibrillin-1 in the kidney is facilitated by the IGF-IR was provided in a model of STZ-induced type 1 diabetes mellitus in *Dcn*$^{-/-}$ and *Dcn*$^{+/+}$ mice. STZ-injected animals developed clinical signs of diabetes mellitus, such as hyperglycemia, proteinuria, and renomegaly, with the only genotype-specific difference concerning higher levels of proteinuria in diabetic *Dcn*$^{-/-}$ compared with *Dcn*$^{+/+}$ mice (Table 1). As expected, nine weeks of diabetes resulted in enhanced glomerular and tubular matrix accumulation. However, morphometrical evaluation of immunostainings for collagen type I and fibronectin did not reveal any genotype-specific differences between diabetic mice (data not shown). Inter-

estingly, *Dcn* deficiency in diabetic kidneys caused lower deposition of fibrillin-1 in comparison with diabetic $Dcn^{+/+}$ mice as shown by quantification of Western blots for fibrillin-1 expression in whole-kidney homogenates (Figure 8, A and B). Moreover, lower deposition of fibrillin-1 in diabetic kidneys from $Dcn^{-/-}$ compared with $Dcn^{+/+}$ mice was associated with enhanced expression of IGF-IR (Figure 8, C and D, Western blot analysis). Thus, *Dcn* deficiency in diabetic kidneys leads to lower expression of fibrillin-1 and up-regulation of the IGF-IR, the latter finding probably representing a compensatory mechanism for the lack of DCN.

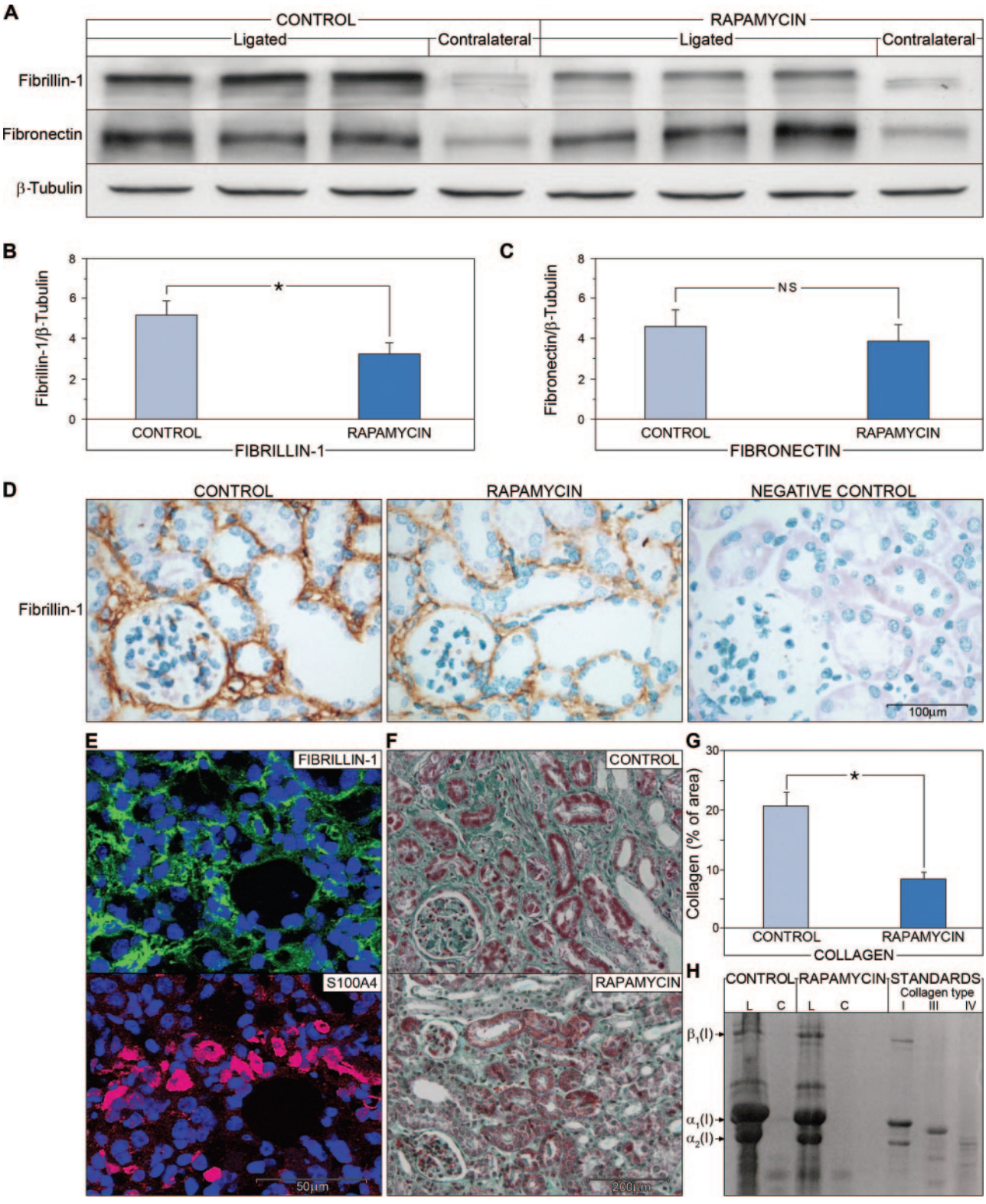

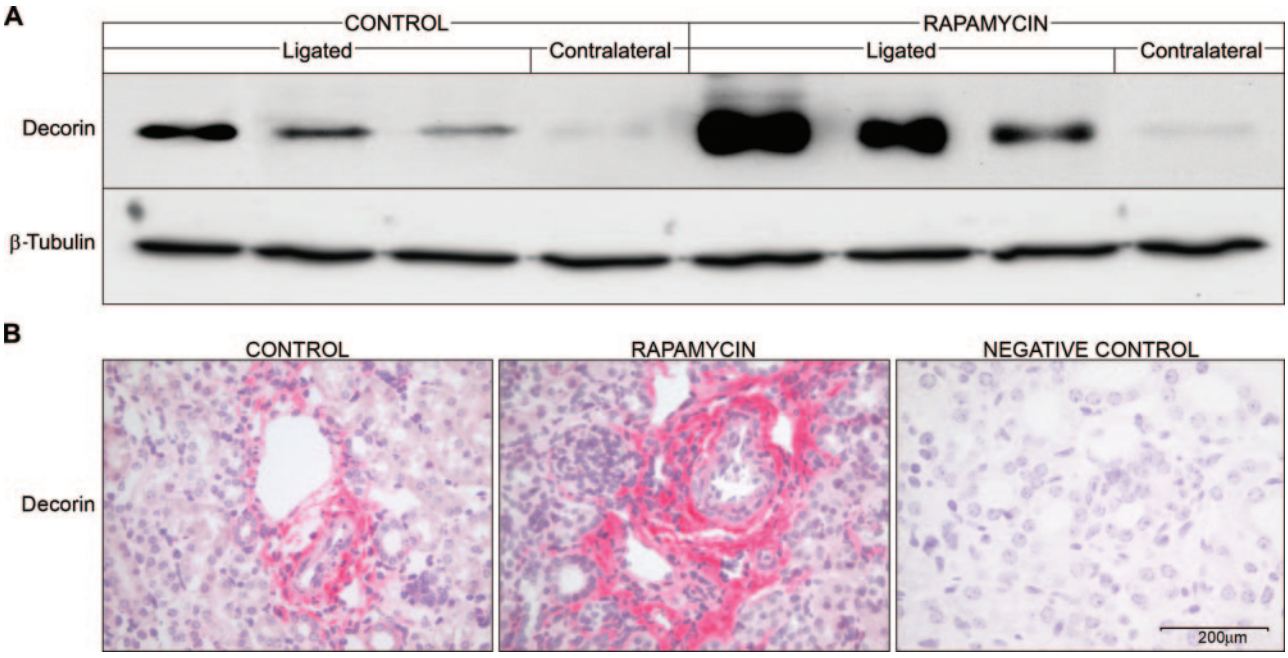

Figure 7. Overexpression of DCN in ligated kidneys from rapamycin-treated mice at day 7 after UUO. **A:** Western blot for DCN core protein after semipurification of ligated and contralateral kidneys from control and rapamycin-treated mice with subsequent digestion of the glycosaminoglycan chain. β-Tubulin is shown as control. **B:** Immunostaining for decorin (alkaline phosphatase anti-alkaline phosphatase, red) in ligated kidneys from control and rapamycin-treated mice indicates increased accumulation of DCN after mTOR inhibition with rapamycin. Counterstaining was with Mayer's hemalaun. The negative control was performed by omitting the primary antibody. Scale bar = 200 μm.

Discussion

In the present study, we report a novel mechanism of action that involves two key molecules: decorin, a small leucine-rich proteoglycan, and the IGF-IR. These two players, together with the downstream signaling pathway evoked by decorin-mediated activation of the receptor, lead to an enhanced translation of fibrillin-1 and its deposition in the extracellular environment both *in vitro* and *in vivo*. Obviously, the control of the IGF-IR by a secreted proteoglycan has implications in the pathophysiology of several renal diseases in which the interstitium is affected by inflammatory and immune responses. A working model depicting some of the major pathways involved in this process and summarizing the main findings of our study is shown in Figure 9.

The biological importance of the model is exemplified by *in vivo* studies of renal injury induced by UUO. In this case, there was overexpression of DCN and fibrillin-1 in wild-type mice, whereas the absence of DCN resulted in reduced up-regulation of fibrillin-1 in obstructed kidneys, giving rise to severe structural damage of the renal parenchyma.[20] In the present study, we confirm and expand this knowledge by delineating the signaling pathway(s) involved in decorin-mediated regulation of fibrillin-1 in the kidney. Decorin-evoked synthesis of fibrillin-1 is abrogated by inhibition of the IGF-IR tyrosine kinase in renal fibroblasts, indicating for the first time the involvement of IGF-IR in the DCN-dependent regulation of fibrillin-1 synthesis. We further show for the first time a direct physical association between human recombinant decorin and the IGF-IR using both co-immunoprecipitation and binding assays. The latter show a high-affinity (K_D ~8 nmol/L) interaction between decorin and IGF-IR. This is consistent with the rapid (5 minutes) induction of IGF-IR phosphorylation by decorin using decorin concentrations about 20 times lower than those required in endothelial cells.[11] Although, the involvement of other receptors (ie, the EGFR or ErbB4[8–10]) cannot be totally excluded at this time, the failure to block the decorin-induced response by specific EGFR inhibitors suggests

Figure 6. In vivo effects of rapamycin on renal accumulation of fibrillin-1 protein 7 days after UUO. **A:** Western blots for fibrillin-1 (**top**) and fibronectin (**middle**) in homogenates of ligated and contralateral kidneys from control and rapamycin-treated mice. β-Tubulin (**bottom**) is shown as control. Semiquantification of Western blots for fibrillin-1 (**B**) and fibronectin (**C**) normalized to β-tubulin in ligated kidneys from control and rapamycin-treated mice. Data are given as means ± SD of the ratios of optical density for fibrillin-1 (**B**) or fibronectin (**C**) to β-tubulin. The **asterisk** indicates statistical significance; $n = 3$, $P < 0.05$. **D:** Immunostaining for fibrillin-1 (peroxidase, brown) in ligated kidneys from control and rapamycin-treated mice indicates a lower intensity of staining in rapamycin-treated kidneys. Counterstaining was with methyl green. The negative control for immunostaining of fibrillin-1 was performed by omitting the primary antibody. **E:** Immunostaining for fibrillin-1 (green) and for fibroblast-like cells (S100A4, red) on serial sections from untreated, ligated kidneys indicated a close spatial proximity of fibrillin-1 to fibroblast-like cells, probably representing fibrillin-1 secreted from fibroblasts and incorporated into extracellular networks. **F:** The Masson trichrome staining indicates less accumulation of collagenous connective tissue (green) in ligated kidneys after administration of rapamycin, compared with ligated kidneys of untreated animals. **G:** Semiquantification of areas of collagen deposition (green, %) in ligated kidneys from rapamycin-treated and control mice. **H:** SDS-polyacrylamide gel electrophoresis gels (4 to 12.5%) under reducing conditions of minced, pepsin-digested whole kidneys and pepsin-digested purified collagen type I, III, and IV standards. The figure shows one of three sample pairs from ligated (L) and contralateral (C) kidneys from rapamycin-treated and control mice. **Arrows** indicate Coomassie Blue-stained bands of α1(I)-, α2(I)-, and β(I)-chains of type I collagen. Scale bars in **D**, **E**, and **F** indicate magnification.

Table 1. Effects of STZ-Induced Diabetes (9 Weeks) on Kidney Weight, Blood Glucose Levels, and Proteinuria in $Dcn^{+/+}$ and $Dcn^{-/-}$ Mice

	Nondiabetic (n = 6)		Diabetic (n = 6)	
	$Dcn^{+/+}$	$Dcn^{-/-}$	$Dcn^{+/+}$	$Dcn^{-/-}$
Body weight, start (g)	24.2 ± 1.6	25.5 ± 1.4	24.9 ± 1.7	25.1 ± 1.5
Body weight, end (g)	29.3 ± 1.7	28.9 ± 1.6	21.4 ± 1.8*	21.8 ± 1.9†
Kidney weight (mg)	229 ± 18.5	210 ± 17.4	312 ± 36*	329 ± 27†
(Kidney weight/body weight) × 10^3	7.8 ± 0.4	7.3 ± 0.4	14.6 ± 1.2*	15.1 ± 1.3†
Blood glucose (mg/dl)	94 ± 7	98 ± 10	450 ± 69*	425 ± 56†
Proteinuria (mg/mg creatinine)	0.41 ± 0.17	0.44 ± 0.16	1.28 ± 0.29*	2.11 ± 0.38†‡

Data are given as means ± SEM.
*$P < 0.05$ for diabetic $Dcn^{+/+}$ versus nondiabetic $Dcn^{+/+}$ mice.
†$P < 0.05$ for diabetic $Dcn^{-/-}$ versus nondiabetic $Dcn^{-/-}$ mice.
‡$P < 0.05$ for diabetic $Dcn^{-/-}$ versus diabetic $Dcn^{+/+}$ mice.

that in renal fibroblasts, this pathway is not significantly involved. In addition, the EGFR levels in renal fibroblasts are notoriously low compared with normal and transformed epithelial cells.

We further show that DCN activates Akt/PKB in renal fibroblasts. The stimulatory effects of DCN on Akt could be abolished by inhibition of either the IGF-IR tyrosine kinase or its downstream target PI3K. DCN also causes phosphorylation of the PDK1. Thus, these data for the first time show that DCN-mediated phosphorylation of Akt involves canonical IGF-I signaling.[13] Importantly, these signaling events are in fact involved in the regulation of fibrillin-1, because inhibition of PI3K markedly reduces the effects of DCN on fibrillin-1 synthesis.

So far, only anti-apoptotic effects have been attributed to DCN/Akt signaling, and only p21 has been identified as a downstream mediator of this cascade.[11,12,35] However, because DCN-dependent regulation of fibrillin-1 occurs at the translational level, mTOR seems to be a likely mediator downstream of Akt.[15,16] DCN causes phosphorylation of mTOR, whereas inhibition of IGF-IR tyrosine kinase or PI3K as well as inhibition of mTOR (by rapamycin) results in a marked reduction of this activation. In keeping with these results, rapamycin reduces DCN-dependent synthesis of fibrillin-1 in renal fibroblasts, providing evidence for the DCN/mTOR-mediated regulation of this molecule. Our results reveal a new level of complexity in the interactions and regulatory functions of matrix constituents, namely the direct regulation of a matrix component (fibrillin-1) by another matrix molecule (DCN).

We also show that DCN induces phosphorylation of p70 S6K at Thr389,[15,16] a downstream translational mediator of mTOR, and this most closely correlates with p70 S6K activity *in vivo*.[41] As expected, DCN-mediated phosphorylation of p70 S6K is abolished by inhibition of either IGF-IR tyrosine kinase or by blockade of PI3K. On the contrary, rapamycin only partially inhibits DCN-mediated phosphorylation of p70 S6K. Because PDK1 is known to phosphorylate p70 S6K either directly or via induction of

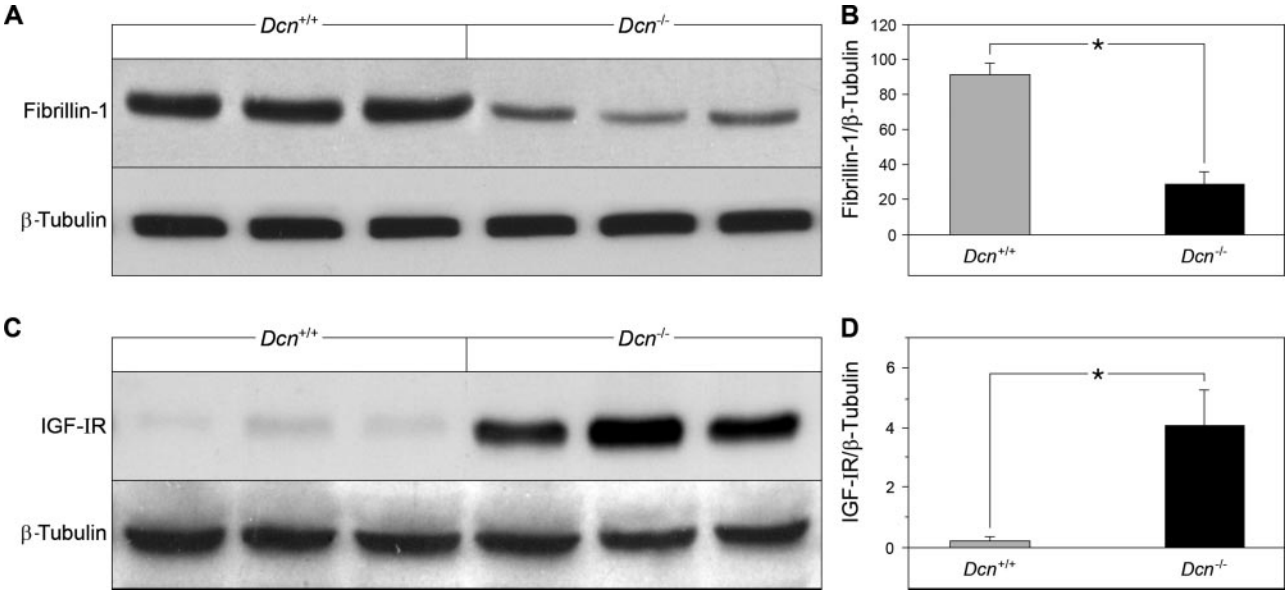

Figure 8. Decorin deficiency in STZ-induced diabetes is associated with lower accumulation of fibrillin-1 and overexpression of IGF-IR. **A** and **C:** Western blots for fibrillin-1 (**A**), IGF-IR (**C**), and β-tubulin in homogenates of diabetic kidneys from $Dcn^{-/-}$ and $Dcn^{+/+}$ mice 9 weeks after induction of diabetes. **B** and **D:** Semiquantification of Western blots of fibrillin-1 (**B**) and IGF-IR (**D**) normalized to β-tubulin in diabetic kidneys from $Dcn^{-/-}$ and $Dcn^{+/+}$ mice 9 weeks after induction of diabetes. Data are given as means ± SD of the ratios of optical density for fibrillin-1 (**B**) or IGF-R (**D**) to β-tubulin. The **asterisk** indicates statistical significance; $n = 3$, $P < 0.05$.

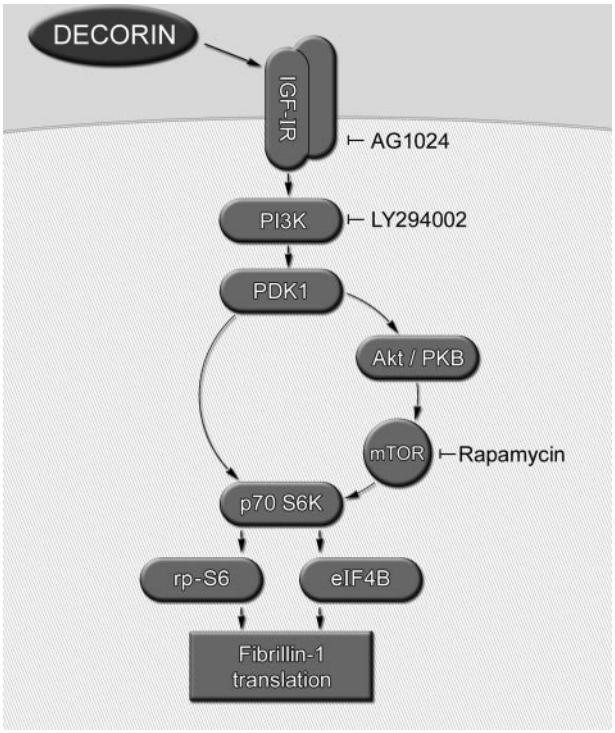

Figure 9. Schematic diagram of the DCN-mediated translational regulation of fibrillin-1 in NRK cells. Further details are given in Results.

PKCζ[16,19] and because DCN leads to an activation of this kinase, PDK1 is the most likely candidate responsible for DCN-mediated, mTOR-independent phosphorylation of p70 S6K. Therefore, it is conceivable that rapamycin only partially inhibits DCN-dependent enhancement of fibrillin-1 synthesis in renal fibroblasts. Moreover, our data indicate direct involvement of PDK1 in the regulation of p70 S6K rather than a PKC-mediated regulatory effect, because DCN and IGF-I had no influence on the phosphorylation of PKCζ. The involvement of p70 S6K in the DCN-dependent regulation of fibrillin-1 is further strengthened by the observation that both translational regulators of protein synthesis eIF4B and rp-S6,[42] located downstream to p70 S6K, are activated by DCN as well. In summary, DCN stimulates fibrillin-1 synthesis by concurrent activation of p70 S6K through the Akt/mTOR pathway and directly via PDK1.

The biological relevance of the mechanisms discussed above is further underlined by results from mice subjected to UUO and rapamycin treatment. There was a reduction in fibrillin-1 protein content in ligated kidneys after rapamycin treatment compared with those from untreated animals. This is probably caused both by a decline in the number of interstitial fibroblast-like cells and by a reduction in production of fibrillin-1 per fibroblast because of the mTOR inhibition. Despite the complexity of this experimental model, UUO has been widely used to study the pathogenesis of tubulointerstitial fibrosis, because the evolution of fibrosis after ureteral obstruction is highly reproducible and reflects the sequence of pathogenetic events in an accelerated manner.[43–45] In UUO, rapamycin leads to a reduction in size and weight of obstructed kidneys due to inhibition of proliferation of tubular epithelial cells and interstitial fibroblasts and to lower deposition of collagen, in agreement with previous studies.[46–49] Furthermore, rapamycin-mediated reduction of fibrillin-1 deposition is not due to a general inhibition of protein synthesis, because fibronectin content is not influenced by rapamycin and DCN deposition.[18,50,51] The pronounced deposition of DCN after administration of rapamycin probably represents a compensatory mechanism in response to inhibition of mTOR. Thus, the reduction of fibrillin-1 deposition in obstructed kidneys, both after inhibition of mTOR and in mice deficient for DCN,[20] implies that the DCN/mTOR-mediated regulation of fibrillin-1 synthesis might be relevant *in vivo* as well.

In a second model of renal injury, type 1 diabetes was induced in mice by STZ to investigate the *in vivo* relevance of DCN/IGF-IR interaction in the regulation of fibrillin-1. Induction of diabetes in $Dcn^{-/-}$ results in lower deposition of renal fibrillin-1 compared with $Dcn^{+/+}$ mice. Simultaneously, the IGF-IR is up-regulated to a higher degree in diabetic $Dcn^{-/-}$ kidneys, probably representing a compensatory mechanism for the lack of DCN but being insufficient to normalize renal fibrillin-1 content.

Our results also explain previous observations that DCN mRNA and protein expression are markedly reduced in patients with severe forms of Marfan's syndrome.[21,22] Although fibrillin-1 mRNA is not altered in these patients, the amount of fibrillin-1 deposited in the extracellular matrix is clearly reduced.[22] In light of our results, these observations can be explained by a mechanism by which reduced levels of DCN signaling through the IGF-IR/Akt/mTOR/p70 S6K pathway would result in a translational down-regulation of fibrillin-1 protein expression. Inter- and intrafamilial phenotypic variability is a common feature of Marfan's syndrome, suggesting that additional modifiers play a role in the pathogenesis of the disease. Our results, together with the previously reported data,[21,22] strongly suggest that DCN could play a significant role as a disease modifier in Marfan's syndrome and perhaps in other type-I fibrillinopathies.

Collectively, our findings show that DCN, by signaling through the IGF-IR and the PI3K/Akt/mTOR/p70 S6K pathway, mediates translational regulation of fibrillin-1. This observation further extends our knowledge of the biology of DCN in two ways: 1) It confirms that the matrix component DCN acts as a signaling molecule through the canonical IGF signaling cascade, and 2) it offers the novel concept that a matrix component (DCN) directly regulates the synthesis of another matrix constituent (fibrillin-1).

Acknowledgments

The technical support of Gabriele Römer and Siegmund Budny is highly appreciated.

References

1. Iozzo RV: The biology of the small leucine-rich proteoglycans: functional network of interactive proteins. J Biol Chem 1999, 274:18843–18846

2. Reed CC, Iozzo RV: The role of decorin in collagen fibrillogenesis and skin homeostasis. Glycoconj J 2003, 19:249–255
3. Danielson KG, Baribault H, Holmes DF, Graham H, Kadler KE, Iozzo RV: Targeted disruption of decorin leads to abnormal collagen fibril morphology and skin fragility. J Cell Biol 1997, 136:729–743
4. Hildebrand A, Romaris M, Rasmussen LM, Heinegard D, Twardzik DR, Border WA, Ruoslahti E: Interaction of the small interstitial proteoglycans biglycan, decorin and fibromodulin with transforming growth factor beta. Biochem J 1994, 302:527–534
5. Border WA, Noble NA, Yamamoto T, Harper JR, Yamaguchi Y, Pierschbacher MD, Ruoslahti E: Natural inhibitor of transforming growth factor-beta protects against scarring in experimental kidney disease. Nature 1992, 360:361–364
6. Schaefer L, Raslik I, Gröne HJ, Schönherr E, Macakova K, Ugorcakova J, Budny S, Schaefer RM, Kresse H: Small proteoglycans in human diabetic nephropathy: discrepancy between glomerular expression and protein accumulation of decorin, biglycan, lumican, and fibromodulin. FASEB J 2001, 15:559–561
7. Kresse H, Schönherr E: Proteoglycans of the extracellular matrix and growth control. J Cell Physiol 2001, 189:266–274
8. De Luca A, Santra M, Baldi A, Giordano A, Iozzo RV: Decorin-induced growth suppression is associated with up-regulation of p21, an inhibitor of cyclin-dependent kinases. J Biol Chem 1996, 271: 18961–18965
9. Patel S, Santra M, McQuillan DJ, Iozzo RV, Thomas AP: Decorin activates the epidermal growth factor receptor and elevates cytosolic Ca2+ in A431 carcinoma cells. J Biol Chem 1998, 273:3121–3124
10. Santra M, Reed CC, Iozzo RV: Decorin binds to a narrow region of the epidermal growth factor (EGF) receptor, partially overlapping but distinct from the EGF-binding epitope. J Biol Chem 2002, 277:35671–35681
11. Schönherr E, Sunderkotter C, Iozzo RV, Schaefer L: Decorin, a novel player in the insulin-like growth factor system. J Biol Chem 2005, 280:15767–15772
12. Schönherr E, Levkau B, Schaefer L, Kresse H, Walsh K: Decorin-mediated signal transduction in endothelial cells: involvement of Akt/protein kinase B in up-regulation of p21(WAF1/CIP1) but not p27(KIP1). J Biol Chem 2001, 276:40687–40692
13. Vincent AM, Feldman EL: Control of cell survival by IGF signaling pathways. Growth Horm IGF Res 2002, 12:193–197
14. Shahbazian D, Roux PP, Mieulet V, Cohen MS, Raught B, Taunton J, Hershey JW, Blenis J, Pende M, Sonenberg N: The mTOR/PI3K and MAPK pathways converge on eIF4B to control its phosphorylation and activity. EMBO J 2006, 25:2781–2791
15. Wullschleger S, Loewith R, Hall MN: TOR signaling in growth and metabolism. Cell 2006, 124:471–484
16. Granville CA, Memmott RM, Gills JJ, Dennis PA: Handicapping the race to develop inhibitors of the phosphoinositide 3-kinase/Akt/mammalian target of rapamycin pathway. Clin Cancer Res 2006, 12:679–689
17. Zhu J, Wu J, Frizell E, Liu SL, Bashey R, Rubin R, Norton P, Zern MA: Rapamycin inhibits hepatic stellate cell proliferation in vitro and limits fibrogenesis in an in vivo model of liver fibrosis. Gastroenterology 1999, 117:1198–1204
18. Shegogue D, Trojanowska M: Mammalian target of rapamycin positively regulates collagen type I production via a phosphatidylinositol 3-kinase-independent pathway. J Biol Chem 2004, 279:23166–23175
19. Romanelli A, Martin KA, Toker A, Blenis J: p70 S6 kinase is regulated by protein kinase Czeta and participates in a phosphoinositide 3-kinase-regulated signalling complex. Mol Cell Biol 1999, 19:2921–2928
20. Schaefer L, Mihalik D, Babelova A, Krzyzankova M, Gröne HJ, Iozzo RV, Young MF, Seidler DG, Lin G, Reinhardt DP, Schaefer RM: Regulation of fibrillin-1 by biglycan and decorin is important for tissue preservation in the kidney during pressure-induced injury. Am J Pathol 2004, 165:383–396
21. Pulkkinen L, Kainulainen K, Krusius T, Makinen P, Schollin J, Gustavsson KH, Peltonen L: Deficient expression of the gene coding for decorin in a lethal form of Marfan syndrome. J Biol Chem 1990, 265:17780–17785
22. Superti-Furga A, Raghunath M, Willems PJ: Deficiencies of fibrillin and decorin in fibroblast cultures of a patient with neonatal Marfan syndrome. J Med Genet 1992, 29:875–878
23. Trask BC, Trask TM, Broekelmann T, Mecham RP: The microfibrillar proteins MAGP-1 and fibrillin-1 form a ternary complex with the chondroitin sulfate proteoglycan decorin. Mol Biol Cell 2000, 11:1499–1507
24. Sterzel RB, Hartner A, Schlotzer-Schrehardt U, Voit S, Hausknecht B, Doliana R, Colombatti A, Gibson MA, Braghetta P, Bressan GM: Elastic fiber proteins in the glomerular mesangium in vivo and in cell culture. Kidney Int 2000, 58:1588–1602
25. Kissin EY, Lemaire R, Korn JH, Lafyatis R: Transforming growth factor beta induces fibroblast fibrillin-1 matrix formation. Arthritis Rheum 2002, 46:3000–3009
26. Bouzeghrane F, Reinhardt DP, Reudelhuber TL, Thibault G: Enhanced expression of fibrillin-1, a constituent of the myocardial extracellular matrix in fibrosis. Am J Physiol Heart Circ Physiol 2005, 289:H982–H991
27. Habashi JP, Judge DP, Holm TM, Cohn RD, Loeys BL, Cooper TK, Myers L, Klein EC, Liu G, Calvi C, Podowski M, Neptune ER, Halushka MK, Bedja D, Gabrielson K, Rifkin DB, Carta L, Ramirez F, Huso DL, Dietz HC: Losartan, an AT1 antagonist, prevents aortic aneurysm in a mouse model of Marfan syndrome. Science 2006, 312:117–121
28. Kenney MC, Zorapapel N, Atilano S, Chwa M, Ljubimov A, Brown D: Insulin-like growth factor-I (IGF-I) and transforming growth factor-beta (TGF-beta) modulate tenascin-C and fibrillin-1 in bullous keratopathy stromal cells in vitro. Exp Eye Res 2003, 77:537–546
29. Tiedemann K, Batge B, Müller PK, Reinhardt DP: Interactions of fibrillin-1 with heparin/heparan sulfate, implications for microfibrillar assembly. J Biol Chem 2001, 276:36035–36042
30. Hausser H, Ober B, Quentin-Hoffmann E, Schmidt B, Kresse H: Endocytosis of different members of the small chondroitin/dermatan sulfate proteoglycan family. J Biol Chem 1992, 267:11559–11564
31. Fisher LW, Stubbs JT III, Young MF: Antisera and cDNA probes to human and certain animal model bone matrix noncollagenous proteins. Acta Orthop Scand Suppl 1995, 266:61–65
32. Kresse H, Liszio C, Schönherr E, Fisher LW: Critical role of glutamate in a central leucine-rich repeat of decorin for interaction with type I collagen. J Biol Chem 1997, 272:18404–18410
33. Schaefer L, Beck KF, Raslik I, Walpen S, Mihalik D, Micegova M, Macakova K, Schönherr E, Seidler DG, Varga G, Schaefer RM, Kresse H, Pfeilschifter J: Biglycan, a nitric oxide-regulated gene, affects adhesion, growth, and survival of mesangial cells. J Biol Chem 2003, 278:26227–26237
34. Glössl J, Beck M, Kresse H: Biosynthesis of proteodermatan sulfate in cultured human fibroblasts. J Biol Chem 1984, 259:14144–14150
35. Schaefer L, Macakova K, Raslik I, Micegova M, Gröne HJ, Schönherr E, Robenek H, Echtermeyer FG, Grassel S, Bruckner P, Schaefer RM, Iozzo RV, Kresse H: Absence of decorin adversely influences tubulointerstitial fibrosis of the obstructed kidney by enhanced apoptosis and increased inflammatory reaction. Am J Pathol 2002, 160:1181–1191
36. Garvey W: Modified elastic tissue-Masson trichrome stain. Stain Technol 1984, 59:213–216
37. Gröne HJ, Cohen CD, Gröne E, Schmidt C, Kretzler M, Schlöndorff D, Nelson PJ: Spatial and temporally restricted expression of chemokines and chemokine receptors in the developing human kidney. J Am Soc Nephrol 2002, 13:957–967
38. Santra M, Eichstetter I, Iozzo RV: An anti-oncogenic role for decorin: down-regulation of ErbB2 leads to growth suppression and cytodifferentiation of mammary carcinoma cells. J Biol Chem 2000, 275:35153–35161
39. Brown EJ, Beal PA, Keith CT, Chen J, Shin TB, Schreiber SL: Control of p70 s6 kinase by kinase activity of FRAP in vivo. Nature 1995, 377:441–446
40. Bascands JL, Schanstra JP: Obstructive nephropathy: insights from genetically engineered animals. Kidney Int 2005, 68:925–937
41. Weng QP, Kozlowski M, Belham C, Zhang A, Comb MJ, Avruch J: Regulation of the p70 S6 kinase by phosphorylation in vivo: analysis using site-specific anti-phosphopeptide antibodies. J Biol Chem 1998, 273:16621–16629
42. Ruvinsky I, Meyuhas O: Ribosomal protein S6 phosphorylation: from protein synthesis to cell size. Trends Biochem Sci 2006, 31:342–348
43. Diamond JR, Ricardo SD, Klahr S: Mechanisms of interstitial fibrosis in obstructive nephropathy. Semin Nephrol 1998, 18:594–602
44. Klahr S: Obstructive nephropathy. Intern Med 2000, 39:355–361
45. Diamond JR: Macrophages and progressive renal disease in experimental hydronephrosis. Am J Kidney Dis 1995, 26:133–140
46. Dixon R, Brunskill NJ: Activation of mitogenic pathways by albumin in

kidney proximal tubule epithelial cells: implications for the pathophysiology of proteinuric states. J Am Soc Nephrol 1999, 10:1487–1497
47. Pallet N, Thervet E, Le Corre D, Knebelmann B, Nusbaum P, Tomkiewicz C, Meria P, Flinois JP, Beaune P, Legendre C, Anglicheau D: Rapamycin inhibits human renal epithelial cell proliferation: effect on cyclin D3 mRNA expression and stability. Kidney Int 2005, 67:2422–2433
48. Morris RE, Cao W, Huang X, Gregory CR, Billingham ME, Rowan R, Shorthouse RA: Rapamycin (Sirolimus) inhibits vascular smooth muscle DNA synthesis in vitro and suppresses narrowing in arterial allografts and in balloon-injured carotid arteries: evidence that rapamycin antagonizes growth factor action on immune and nonimmune cells. Transplant Proc 1995, 27:430–431
49. Stallone G, Infante B, Schena A, Battaglia M, Ditonno P, Loverre A, Gesualdo L, Schena FP, Grandaliano G: Rapamycin for treatment of chronic allograft nephropathy in renal transplant patients. J Am Soc Nephrol 2005, 16:3755–3762
50. Svegliati-Baroni G, Ridolfi F, Di Sario A, Saccomanno S, Bendia E, Benedetti A, Greenwel P: Intracellular signaling pathways involved in acetaldehyde-induced collagen and fibronectin gene expression in human hepatic stellate cells. Hepatology 2001, 33:1130–1140
51. Kim MS, Park J, Ha H, Kim YS, Kang SW, Jeong HJ, Kang DH, Yang CW: Rapamycin inhibits platelet-derived growth factor-induced collagen, but not fibronectin, synthesis in rat mesangial cells. Yonsei Med J 2004, 45:1121–1126